JOURNAL OF CATALYSIS 141, 660–670 (1993)

Preparation and EXAFS Studies of Highly Dispersed Iron Catalyst Derived from $Fe_3(CO)_{12}$ Precipitated on Alumina

YUAN KOU,* HONG-LI WANG,* MURE TE,* TSUNEHIRO TANAKA,† AND MASAHARU NOMURA‡

*State Key Laboratory for Oxo Synthesis and Selective Oxidation (OSSO), Lanzhou Institute of Chemical Physics, Chinese Academy of Sciences, Lanzhou 730000, China; †Department of Hydrocarbon Chemistry and Division of Molecular Engineering, Kyoto University, Kyoto 606, Japan; and ‡Photon Factory, National Laboratory for High Energy Physics, Tsukuba 305, Japan

Received May 7, 1992; revised December 2, 1992

Supported tri-iron dodecacarbonyl has been prepared by a novel method, precipitating the cluster on alumina without any pretreatment. The precipitated $Fe_3(CO)_{12}/Al_2O_3$ retains a molecular structure similar to that of its parent compound as demonstrated by Fe *K*-edge XANES (*X*-ray *a*bsorption *n*ear-*e*dge *s*tructure) and infrared results. After decarbonylation under very mild conditions (310 K in vacuum), the Fe/Al_2O_3 obtained exhibits a good catalytic selectivity for lower olefins in the hydrogenation of carbon monoxide. *K*-edge EXAFS (*e*xtended *X*-ray *a*bsorption *f*ine *s*tructure) analyses of the fresh catalyst and the used catalyst suggest that the active site on the surface is an ensemble of three iron atoms with one short Fe–Fe bond of 2.52 ± 0.05 Å and two longer Fe–Fe bonds of 2.74 ± 0.04 Å. However, the aggregation of these Fe_3 groups to particles over 10 Å in size brings about a short lifetime and poor selectivity for the catalyst. The aggregated particles are still two-dimensional, consisting of at least three iron trimers in which the interatomic distance for each trimer of iron on the average is 2.48 ± 0.08 Å, and the nearest interatomic distance between two trimers is 2.83 ± 0.03 Å.

I. INTRODUCTION

The use of tri-iron dodecacarbonyl as the precursor for preparing a metallic iron catalyst has proved to be very successful for hydrogenation of CO to lower olefins (*1*, *2*). However, neither the preparation of supported clusters for this system nor the characterization of fine particles on the surface derived therefrom have received sufficient attention. In general, it may be assumed that the equilibria between metallic particles and carbonyl clusters in such systems are reversible under certain conditions, and insight into some aspects of the catalytic mechanism on the surface may be gained by studying either the precursor of the catalyst or its derivatives (*3*). Characterization of both the structure and the surface chemistry of the supported cluster is required for this purpose. However, it is very difficult to reach the point that the direct evidence obtained is completely satisfactory. This is brought about by the following reasons. (i) The most widely used technique in the preparation of supported iron clusters begins with impregnating the oxide supports with a solution of $Fe_3(CO)_{12}$. Such a procedure is easy in operation, but the product obtained strongly depends upon the pretreatment of the supports because of cluster–support interactions. For example, impregnation of Al_2O_3 with $Fe_3(CO)_{12}$ cannot produce $Fe_3(CO)_{12}/Al_2O_3$ unless 0.2 *M* HCl is added or Fe loading exceeds 2 wt% (*4*). The cluster–support interaction that occurs immediately during the experiment not only limits the observation, but also causes a poor reproducibility in the preparation of highly dispersed catalyst. Therefore, it is difficult to judge whether the different results observed are due to the difference in preparation or not. (ii) Cluster-derived iron catalysts exhibit relatively high selectivity

0021-9517/93 $5.00

for lower olefins in CO hydrogenation, but the life of the catalyst is usually short (*1*). Although the aggregation to particles over 10 Å is thought to cause poor selectivity, well-defined structural evidence from the support surface is still lacking because of the technical difficulties in the characterization involved.

Preparation of the supported cluster by impregnation is generally not satisfactory, especially when high dispersion is desired and acidic oxides are used (*5*). A convenient and superior method of directly precipitating $Fe_3(CO)_{12}$ onto γ-Al_2O_3 with an aqueous solution of the intermediate obtained from a conventional synthetic route of $Fe_3(CO)_{12}$ (*6*) is presented in this work. By this method, the metal loading can be controlled quantitatively by varying the concentration of the intermediate solution at the initial stage of the process. Based upon the significantly improved reproducibility, the work presented here focuses on the relationship between carbonyl clusters and highly dispersed iron particles on the surface. The recent development in the theoretical calculation of EXAFS (*e*xtended *X*-ray *a*bsorption *f*ine *s*tructure), FEFF code (*7*, *8*), allows us to determine these extremely small units in detail with good accuracy.

II. EXPERIMENTAL

Preparation of Iron Carbonyl

$Fe_3(CO)_{12}$ was prepared by the literature method (*6*), identified by IR spectra, and maintained in a flask under an inert atmosphere. The $Fe_3(CO)_{12}$ studied here was unpurified in line with the precipitated $Fe_3(CO)_{12}$ in the supported samples prepared as described below.

Preparation of $Fe_3(CO)_{12}/\gamma$-Al_2O_3 by Precipitation

All the operations were carried out under the protection of nitrogen.

Preparation of the intermediate solution. To 11 ml $Fe(CO)_5$ (industrial grade) in 45 ml of dry CH_3OH, 11 g NaOH in 25 ml of distilled water was added. The mixture was stirred for about 30 min, then 32 ml of saturated NH_4Cl solution was added dropwise. A freshly prepared MnO_2 suspension (17 g $KMnO_4$/75 ml H_2O + 25 ml 95% C_2H_5OH) was added, stirred for about 2 h, then 10 g $FeSO_4 \cdot 7H_2O$ in 60 ml 4 *M* H_2SO_4 was added carefully. The settled solution maintained under nitrogen, the color of which had changed to purplish red, was used as the intermediate. The concentration of the clear intermediate solution was calculated to be 0.013 g Fe/ml based on the yield.

Preparation of $Fe_3(CO)_{12}/\gamma$-Al_2O_3. The γ-alumina (industrial grade, 0.707 g/ml, Wenzhou Chemical Industry) was unpretreated but purged by purified N_2. The BET surface was 160–170 m^2/g. The average pore diameters were in the range 30–50 Å. The typical preparation of 1.1 wt% Fe loading supported cluster was as follows. Under the protection of nitrogen, 6 *M* HCl was added to 3 ml of the above purplish red, clear intermediate solution until pH 2–3, at which point the solution was still clear and no precipitation was found on the flask wall. The 5 ml Al_2O_3 (particle size 40–60 μm) was impregnated by the intermediate solution for about 30 min, then washed in 5 ml of 0.2 *M* HCl. The color changed to pale green immediately. After decanting the remaining liquid phase, the sample was washed in 0.3 *M* K_2CO_3 until pH 8 in the filtrate and dried in vacuum at 300 K for 10 h. Several samples of $Fe_3(CO)_{12}/Al_2O_3$ with different metal loadings were prepared by controlling the concentration of HCl prior to impregnating the alumina. All samples were checked by Mn *K*-edge EXAFS to ensure that no manganese remained on the surface.

Spectral Measurement

Infrared spectra were recorded on a Fourier Transform Nicolet 10DX spectrometer using a Nujol mull for pure $Fe_3(CO)_{12}$ and pressed disks for $Fe_3(CO)_{12}/Al_2O_3$.

X-ray absorption spectra were obtained using the BL-10B and BL-7C facilities at the Photon Factory (Tsukuba, Japan) with a positron beam energy of 2.5 GeV and an

average stored current of 250 mA. Data for pure carbonyl were collected on the BL-10B experimental station with a Si(311) channel-cut monochromator in transmission mode using ion chambers with N_2 and Ar fill gas, and supported samples were measured on the BL-7C station with a Si(111) double-crystal (sagittal focusing) monochromator in fluorescence mode. Spectra were recorded in four energy regions about the Fe K-edge, -100 to -30 eV in 15-eV steps, -30 to 70 eV in 0.5-eV steps, 70 to 700 eV in 4-eV steps, and above 700 eV in 8-eV steps. The signal was integrated for 4 s at each point. The energy calibration was set as 7111.0 eV at the Fe foil $3d$ near-edge feature. $Fe_3(CO)_{12}/Al_2O_3$ was measured in both modes to calibrate the edge positions. In the transmission mode, a specimen of pure carbonyl maintained under N_2 was made by simply applying the powders (<30 μm) on Scotch tape. About six layers of tape were used to fabricate samples with $\Delta\mu x$ of 1.2, where μ is the linear absorption coefficient and x is the sample thickness. Specimens of supported samples maintained under N_2 were made by powdering, then pressing into discs. A thickness of about 1.5 mm was used to fabricate samples with $\Delta\mu x$ of 0.3. In the fluorescence mode, specimens also maintained under N_2 were made by directly applying the fine powders on the tape. All specimens were prepared inside a glove box kept under an atmosphere of nitrogen, sealed by the tape, then measured immediately.

Data Analysis

The data was processed on a SUN386/P9 microcomputer with the Program Library for EXAFS Data Processing written by the Institute of Physics, Chinese Academy of Sciences. The photon energy of the raw data was converted to the photoelectron wave vector k, the background was subtracted by fitting and extrapolating the pre-edge region (-50 to -20 eV) by Victoreen's formula. The XANES (*X*-ray *a*bsorption *n*ear-*e*dge *s*tructure) data were normalized within 70 eV (-20 to 50 ev) about the edge to give an absorption jump of 1.0. The E_T was taken at the maximum in the first derivative of the Fe $3d$ feature. The EXAFS data were normalized by a smooth spline μ_0, determined by a cubic spline fit from the continuum above the edge to about 900 eV. The EXAFS oscillation $\chi(k)$ was determined by $\chi(k) = (\mu - \mu_0)/\mu_0$. The $k^3\chi(k)$ was Fourier transformed into r-space by a Hanning window function. The first point transformed, k_{min}, was chosen at the minimum behind the multiple scattering peak, which appeared in the XANES region, and the last point, k_{max}, finally determined by the number of fit parameters N_{idp}, $N_{idp} < 2\Delta k\Delta R/\pi$ (9), in which $\Delta k = k_{max} - k_{min}$ and $\Delta R = R_{max} - R_{min}$ is the width of the Hanning window in r-space. The procedures were checked several times with different spline parameters and within different k-space, generally reproduced in the range $k = 3.5$ to 12.0 to make sure that the Fourier transforms obtained for each sample had uniform spectral features.

The Fourier transform containing all the significant peaks was then filtered into k-space between R_{min} and R_{max} (generally about 0.7 and 3.0, respectively), by which the peaks of interest were perfectly resolved from the remainders. Thus, the experimental EXAFS data $\chi_E(k)$ were obtained. A least-squares curve-fitting procedure then was performed to calculate the parameters for each shell using theoretically calculated components determined by the Program FEFF3.25 developed by Professor J. J. Rehr and his colleagues at the University of Washington with their permission. The structural parameters (coordination number, CN; shell radius, R in angstrom; Debye–Waller factor DW in angstrom squared) with which the program was started referred to the single-crystal values. They were corrected repeatedly until they were identical to the fitting parameters. The reduction factor used, S_0^2, is 1.1. The best fit of fitting

curve $\chi_T(k)$ to $\chi_E(k)$ was first chosen by an R-factor,

$$R = \left| \frac{(\chi_T(k) - \chi_E(k))^2}{\chi_E(k)^2} \right|^{1/2},$$

then was transformed into r-space weighted by k^0 within the same range to give a fit of the Fourier transform. Comparing the fit with the Fourier transform by much the same spectral features gives an opportunity to further check the R-factor and to finally determine the best fit of $k^3\chi(k)$. These procedures have a distinct advantage in avoiding the doubtful explanation of EXAFS derived data especially in the case that many variables, about 13 in total, are involved in the unknown systems. The EXAFS derived data were also checked by and compared with the fitting result of $k^3\chi(k)$ filtered from the first peak appearing on the Fourier transform.

The parameter error estimates were calculated by the recommended method (*10*). The correlations between the variables were estimated by the standard method (*11*).

III. RESULTS AND DISCUSSION

Formation of $Fe_3(CO)_{12}/Al_2O_3$ by precipitation. The preferred methods (*12*) of preparation of $Fe_3(CO)_{12}$ involve the oxidation of $HFe_3(CO)_{11}^-$ by strong acid, or the oxidation of $HFe(CO)_4^-$ by MnO_2 (*12*). In the latter case (6), the direct product is not $Fe_3(CO)_{12}$ but a mixed intermediate. When the mixture is settled for a while before pouring, a rosy colored solution is obtained. Then $Fe_3(CO)_{12}$ can be precipitated immediately when 9 M H_2SO_4 is added to the solution, i.e.,

$$3HFe(CO)_4^- + 3MnO_2 + 3H_2O \xrightarrow[\text{settling}]{\text{after}} \text{solution} \xrightarrow{H^+} Fe_3(CO)_{12}\downarrow + 3Mn^{2+} + 9OH^-. \quad (1)$$

The preparation of $Fe_3(CO)_{12}/Al_2O_3$ by precipitation begins with impregnating Al_2O_3 with the rosy colored solution. After 0.2 M HCl was added, the rosy colored

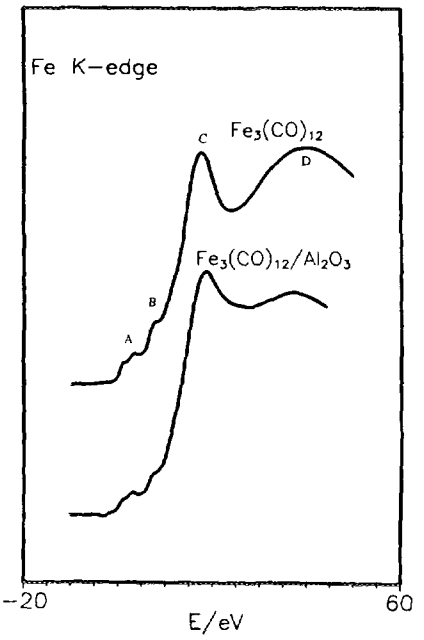

FIG. 1. Fe K-edge XANES spectra of $Fe_3(CO)_{12}$ and $Fe_3(CO)_{12}/Al_2O_3$.

Al_2O_3 when impregnated to saturation changed to green immediately. A similar phenomenon has been observed previously when aqueous HCl was added to $HFe_3(CO)_{11}^-/Al_2O_3$ (*13*). It is visual evidence for the formation of $Fe_3(CO)_{12}$ on the surface.

The supported samples have the characteristic green color of the parent cluster. The freshly prepared samples show infrared absorptions at 2107(*w*), 2048(*s*), 2018s(*br*), 1998(*sh*), and 1825(*m*) cm^{-1}, similar to those for the unpurified $Fe_3(CO)_{12}$ (2108(*sh*), 2048(*s*), 2013s(*br*), 1984(*sh*), 1856(*sh*), and 1825(*m*) cm^{-1}) obtained in our laboratory. The $Fe_3(CO)_{12}$ precipitated on alumina can be extracted from the surface by hexane to give a green solution identified as the parent compound from its infrared spectrum. It provides evidence that the precipitated $Fe_3(CO)_{12}$ is not strongly adsorbed.

Fe K-edge XANES results show that almost all the pre-edge and edge features of $Fe_3(CO)_{12}$ are maintained in the spectrum of $Fe_3(CO)_{12}/Al_2O_3$, as shown in Fig. 1. It is

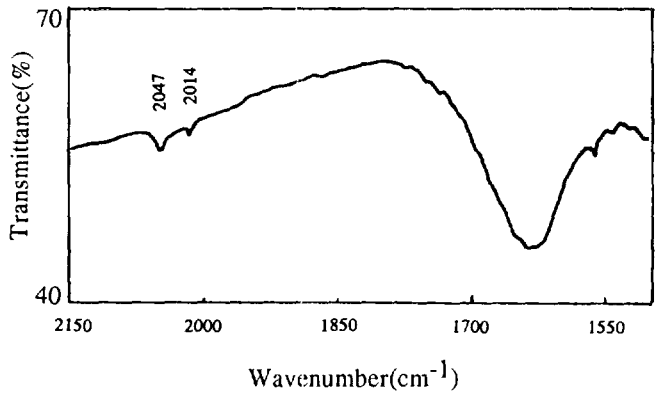

FIG. 2. Infrared spectrum of CO adsorbed on Fe/Al_2O_3.

found, however, that peak B is reduced in intensity and that the energy difference between peaks C and D has decreased. In $Fe_3(CO)_{12}$, only the iron atom unbridged by the carbonyls is exactly six-coordinated. The local symmetry of the other two irons can be described approximately as distorted octahedral. In this case (*14*), the 1*s* to 3*d* transition is weakly allowed, accompanied by the back-donation of the *d* charge, giving a peak A in the pre-edge region. The 4*s* to 3*d* electron transfer generates partly vacant 4*s* orbitals and causes a significant peak B due to the transition of 1*s* to 4*s* character. The 1*s* to 4*p* transition gives the maximum in the spectrum, peak C. Peak D is a unique feature of carbonyls, in which the colinear *M*–C–O array (*M*, metal atom) exists. Similar multiple scattering features were observed in $Fe(II)(CN)_6$ and $Fe(III)(CN)_6$ (*15*) and in $Co(CN)_6^{3+}$ (*16*).

The dispersion process by which the cluster interacts with the surface requires the participation of 4*s* electrons to strengthen the Fe–Fe bonds, and therefore the intensity of peak B in the spectrum of $Fe_3(CO)_{12}/Al_2O_3$ is decreased. As a consequence, the Fe–C bonds are weakened and lengthened, as suggested by the shift of the multiple scattering peak D to lower energy (*15*). In comparison with its parent compound, the energy distance between the threshold E_T and peak D is decreased by 3.1 eV. The more distorted site symmetry is also indicated by the weakened intensity of peak D.

$Fe_3(CO)_{12}/Al_2O_3$ was easy to decarbonylate. The decarbonylation could occur either under very mild conditions or spontaneously under a nitrogen atmosphere.

$Fe_3(CO)_{12}/Al_2O_3$ is not sensitive to air but is very sensitive to temperature. After treating in vacuum up to 310 K, a rapid decoloration occurs. First, the color changes to rose and bright yellow, then to white. The white sample, in which no infrared absorption band due to a carbonyl group was found, seems to be the "final" product obtained from the treatment. When it was treated by continuously raising the temperature, no further color change was observed. This shows that the decoloration in fact is a decarbonylation process that may indicate the formation of highly dispersed iron on alumina.

An attempt to maintain the rosy colored intermediate was unsuccessful because of its very poor stability. An *in situ* infrared study was therefore undertaken.

Maintaining the white sample in CO atmosphere for a few days gives a yellow product and causes the reappearance of three very weak infrared absorption bands centered at 2047, 2014, and 1549 cm^{-1}, shown in Fig. 2. Both the white and the yellow product are quite stable under N_2, show no color change within 10 min on exposure to air,

TABLE 1

Catalytic Activity of Fe/Al_2O_3 Prepared from $Fe_3(CO)_{12}/Al_2O_3$ Pretreated under Different Conditions

No.	Fe (wt%)	Selectivity to light olefins (mol%)	Catalytic activity	Washed by K_2CO_3
K1	0.17		None	No
K2	0.35		None	No
K6	0.70	20.0	Low	No
K9	0.70	77.6	High	Yes
K7	0.90	66.0	High	Yes
K11	0.90	68.5	High	Yes
K13	1.20	88.1	High	Yes
K12	1.50	20.0	High	Yes

Note. Reaction conditions: 2.0-MPa syngas ($CO:H_2 = 1:2$), 473 K, fixed-bed reactor with an *in situ* GC analyzer, GHSV = 600–1000 h^{-1}

but change to a pink-red mixture after a few hours, which might be caused by the formation of iron oxides.

Selectivity of Fe/Al_2O_3 in the catalytic hydrogenation of CO. The results from Table 1 show that the high selectivity of Fe/Al_2O_3 to produce light olefins in the hydrogenation of CO appears in the range 0.7 to 1.2 wt% Fe. Although a high selectivity was reached, the so-called "short-life" problem was still present. For example, after about 2 h, the selectivity of K9 to produce light olefins decreased to 36%, and the conversion was only about 30% of that observed initially. It was also found that reducing the catalysts after use under flowing hydrogen at 520 K was not effective for recovering its selectivity and activity.

Comparing the activity and the selectivity of supported metallic Fe/Al_2O_3 catalysts with those of supported clusters, we note that both exhibit much the same catalytic behavior. When exposing the working catalysts to air at 420 K, both exhibit a similar visible color change from white to pale blue or brown within a few seconds caused by the oxidation of iron particles (*17*).

Surface structure of Fe/Al_2O_3 determined by EXAFS. In order to probe the possible reason for the short-life problem, freshly prepared catalyst Fe/Al_2O_3(K7) was chosen to compare its surface structure with that of the K7 used for EXAFS analysis. $Fe_3(CO)_{12}$ was used as a standard sample for calibrating the fitting parameters in this work. A single-crystal analysis demonstrated that $Fe_3(CO)_{12}$ (*18*) has an iron core that is an isosceles triangle, in which there is a short Fe–Fe bond of length 2.558 Å bridged by two carbonyls, while the longer Fe–Fe bonds unbridged by carbonyl are 2.680 Å. On average, each iron atom is coordinated by 3.3 terminal carbon atoms (C_t) and 1.3 bridging carbons (C_b). An average Fe–C_t bond is 1.82 Å and Fe–C_b is 2.05 Å. *K*-edge EXAFS of solid $Fe_3(CO)_{12}$ was also investigated by theoretical fitting with EXCURV (*19*), but the average Fe–C bond obtained was only about 1.81 Å, much

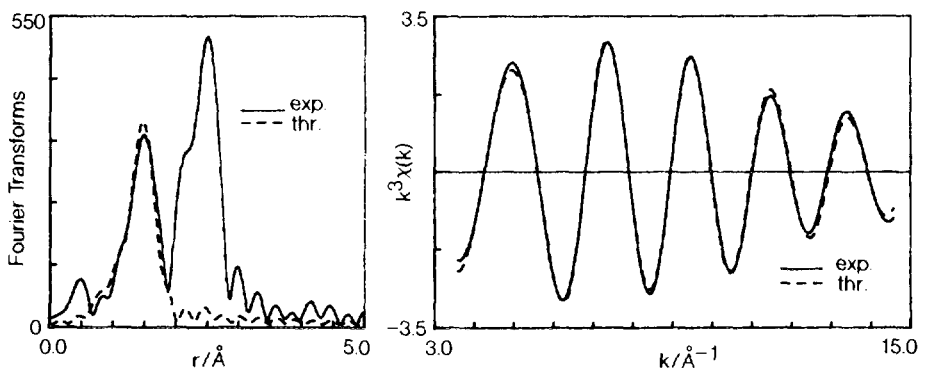

FIG. 3. Fourier transform (left) of $k^3\chi(k)$ of $Fe_3(CO)_{12}$ and the fitting curve (right) to $k^3\chi_1(k)$ filtered from 0.7 to 1.92 on the Fourier transform.

shorter than the average value 1.89 Å based on a single-crystal study. It can be found from the Fourier transform of the Fe *K*-edge EXAFS of $Fe_3(CO)_{12}$ shown in Fig. 3 that the Fe–C shell ranging from 0.7 to 1.92 Å contributes a peak well separated from the others. Fitting the filtered oscillation with two shells of Fe–C_t and Fe–C_b by the use of a S_0^2 factor as 1.1 gives, as shown in Fig. 3, the satisfactory results listed in Table 2.

The spectra of Fig. 4 show that, for the Fourier transforms, the freshly prepared catalyst K7 and the K7 after use exhibit the same feature in the first peak, but a pronounced difference in the second and/or third peaks. The change in position of the second peak is noteworthy, and the second peak in the spectrum of K7 with a relatively high intensity seems to divide into two peaks in the spectrum for K7 after use. The calculated parameters, obtained by fitting the EXAFS data in *k*-space shown in Fig. 4, are listed in Table 3. To make sure that the differences found above are real and can be obtained reproducibly, two freshly prepared samples with different metal loadings were further investigated. The EXAFS parameters derived for these samples are also shown in Table 3, and they can be seen to be very reproducible.

Based on the EXAFS derived parameters, the surface structure of the freshly prepared catalyst can be described as follows. Each iron atom is surrounded by three oxygen atoms provided by alumina, and each one is bonded by one nearest iron atom with the distance of 2.49 to 2.55 Å (2.52 Å on average) and by one next nearest iron with the distance of 2.73 to 2.75 Å (2.74 Å on average). Although the coordination numbers (CN) of these two iron neighbors are very small, the ratio of $CN_{2.52}$ to $CN_{2.74}$ is maintained as a constant 1 : 2 for the different samples studied. In the EXAFS analysis of carbonyl clusters, this is known to be a characteristic of an isosceles triangle cluster core such as the Fe_3 core in $Fe_3(CO)_{12}$.

In principle, the ratio of the CN of the shorter Fe–Fe shell to the CN of the longer one in the Fe_3 core of $Fe_3(CO)_{12}$ should be 0.7 : 1.3 if these two shells were separable by the EXAFS technique. However, in the case of three freshly prepared iron catalysts, the average ratio is 0.3 : 0.7, only one-half of that in $Fe_3(CO)_{12}$. Whether it is caused by the fragmentation of the parent cluster during preparation or the cleavage of the Fe–Fe bond after the decarbonylation still remains an open question, but it is clear that some isolated iron atoms, which cause the third coordination at 2.96 Å with relatively higher CN, are formed and maintained on the surface. A tentative structural model for

TABLE 2

Fe *K*-Edge EXAFS-Derived Coordination Number (CN), Shell Radius (*R*), Debye–Waller Factor (DW) for the Fe–C Bonds in $Fe_3(CO)_{12}$ Unpurified

Shell	Crystal (CN/*R*) (*18*)	CN	*R* (Å)	DW	*R*-factor
Fe–C_t	3.3/1.82(2)	3.1(5)	1.83(1)	0.003	0.08
Fe–C_b	1.3/2.05(3)	1.6(7)	2.07(3)	0.006	

Note. Filtered range (Å), 0.72–1.92; fitting range in *k*-space, 2.7 to 15.0 $Å^{-1}$ with the weight k^3.

TABLE 3

EXAFS-Derived Coordination Numbers (CN), Shell Radii (*R*), and Debye–Waller Factors (DW) of Clusters-Derived Fe/Al_2O_3

Sample (Fe wt%)	Shell	CN	*R* (Å)	DW	*R*-factor
K7(0.9)	Fe–O	2.9(5)	1.97(2)	0.007	0.10
	Fe–Fe	0.3(2)	2.51(5)	0.005	
	Fe–Fe	0.5(3)	2.73(4)	0.005	
	Fe–Fe	1.8(9)	2.96(5)	0.015	
K37(1.1)	Fe–O	2.8(6)	1.95(2)	0.007	0.13
	Fe–Fe	0.4(2)	2.55(5)	0.004	
	Fe–Fe	0.8(4)	2.75(4)	0.006	
	Fe–Fe	2.6(14)	2.97(8)	0.017	
K17(0.6)	Fe–O	2.8(7)	1.97(3)	0.007	0.15
	Fe–Fe	0.3(2)	2.49(5)	0.001	
	Fe–Fe	0.8(5)	2.73(5)	0.006	
	Fe–Fe	2.6(16)	2.95(7)	0.016	
K7 used (0.9)	Fe–O	2.9(7)	1.97(2)	0.007	0.13
	Fe–Fe	2.2(9)	2.48(8)	0.011	
	Fe–Fe	1.9(9)	2.83(3)	0.011	
	Fe–Fe	2.4(11)	3.02(4)	0.012	

Note. Theoretical fitting range in *k*-space, 2.8–12.48 $Å^{-1}$ with the weight of k^3.

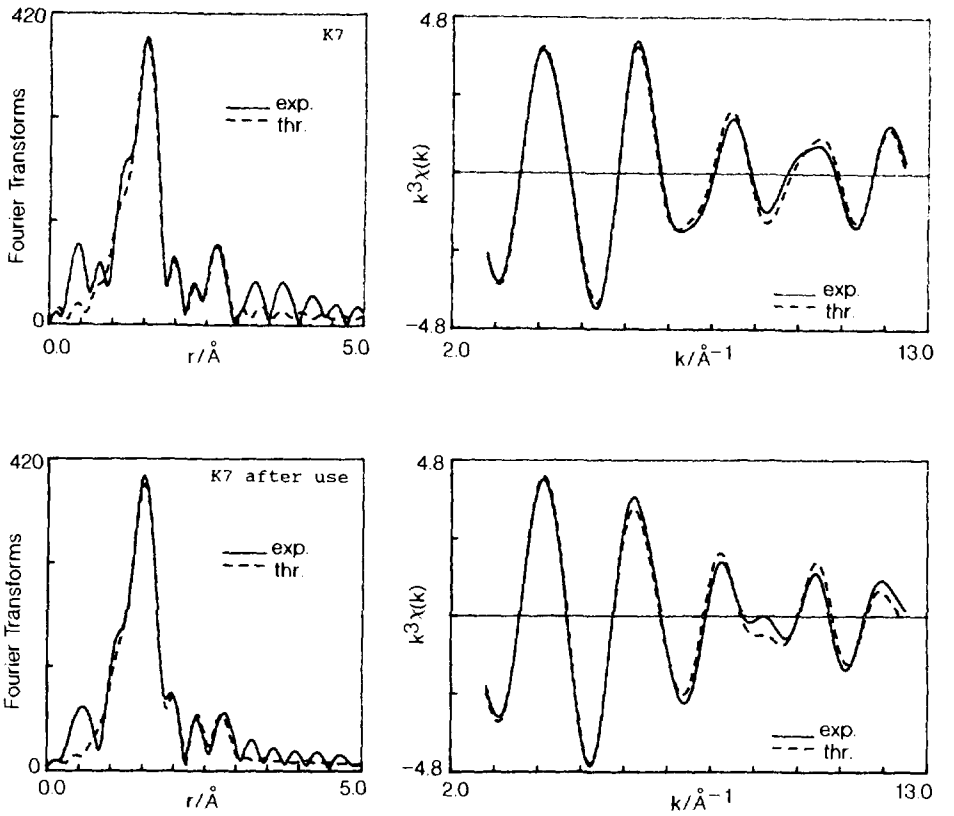

FIG. 4. Fourier transform and fitting curve in k-space of Fe K-edge EXAFS of Fe/Al_2O_3(K7) and K7 after use.

the catalyst Fe/Al_2O_3 is therefore developed based on the above finding and illustrated in Fig. 5. It can be seen in Fig. 5 that there are mainly two species of iron on the surface. One is the randomly distributed isolated atoms, and the other is the tri-iron ensembles, which appear to constitute the catalytic sites under reaction conditions. Similar results, such as separate ensembles consisting of three Os atoms as active centers for CO hydrogenation, were reported for $Os_3(CO)_{12}/Al_2O_3$ in earlier work (*20*). The isolated atoms of Fe are not expected to be catalytically active (*21*). In both cases, however, each iron atom is triple-bridged by three oxygen atoms of alumina; the average angle of the O–Fe–O bonds is calculated to be about 90°, as shown in Fig. 6.

The surface of the small γ-Al_2O_3 particles was reported to be predominantly (111) in orientation (*22–24*), but in more recent literature (*25*, *26*) it was suggested to be (110). For the latter case, the arrangement of such an ensemble of three iron atoms will be expected to be somewhat different from that shown in Figs. 5 and 6, which are produced by assuming for simplicity the surface orientation to be (111). However, it is clear from the EXAFS-derived parameters listed in Table 3 that two iron atoms cannot occupy two adjacent short-bridge sites of lattice oxygen on the (*110*) plane. This is because the distance between them would be too short, only about 2.0 Å. One of the possible arrangements of the tri-iron ensembles on the (110) plane is shown in Fig. 7, in which the

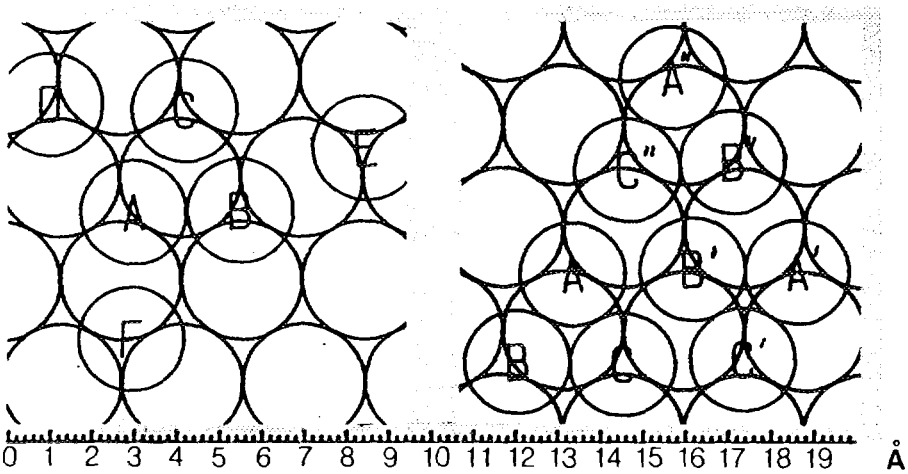

K7

Atom	Coordination Number(CN) $CN_{2.51}$	$CN_{2.73}$
A	1	1
B	1	1
C	0	2
D	0	0
E	0	0
F	0	0
CN for each	0.3	0.7

The subscripts of CN represent the interatomic distances in Å.

K7 after use

Atom	Coordination Number(CN) $CN_{2.48}$	$CN_{2.83}$
A	2	2
B	2	0
C	2	2
A′	2	1
B′	2	4
C′	2	1
A″	2	0
B″	2	2
C″	2	2
CN for each	2.0	1.6

FIG. 5. Tentative models of Fe/Al_2O_3(K7) and K7 after use in accordance with a (111) plane and the EXAFS-derived results listed in Table 3.

second layer of lattice oxygens is not shown for clarity, although it is also involved in the coordination to iron. We can see from Figs. 5 and 7 that the coordination of surface oxygens by the tri-iron species is 3.0 and close to 3 for (111) and (110), respectively. The difference in CN between these two cases cannot be distinguished by EXAFS because of the limitation of the technique. We therefore represent the γ-Al_2O_3 surface in this paper by the (111) plane, but the same conclusions can be drawn likewise with the (110) plane, although the situation in this case is somewhat more complicated.

As to the structure of the used catalyst K7, its first shell as estimated from the Fourier transforms is much the same as that of K7. However, there are significant differences in the second and third shells. The EXAFS-derived results listed in Table 3 suggest that the iron atoms deposited on the surface seem to be in trimers with a distance between the two irons of 2.48 ± 0.08 Å, similar to that observed for K7. The aggregated ensemble is still two-dimensional as demonstrated by its CN of the oxygen shell. It consists of at least three or four iron trimers in which the interatomic distance is 2.48 ± 0.08 Å and the nearest interatomic distance between two adjacent trimers is 2.83 ± 0.03 Å, respectively. Other neighboring iron ensembles and/or atoms give the third coordination at 3.02 Å. A tentative model is shown in Fig. 5. The formation of

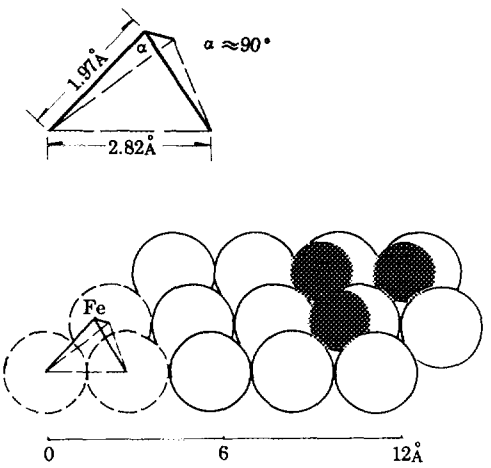

FIG. 6. Calculation of the O–Fe–O angle based on the results of K7 shown in Fig. 5. The first neighbors only are concerned.

such aggregated iron ensembles over 10 Å in size appears to be the cause for short-life and poor selectivity of the catalyst. From the EXAFS-derived results, we can reasonably assume that for the freshly prepared catalyst Fe/Al_2O_3 the dispersed iron atoms tend to come close to each other under reaction conditions and occupy positions coordinated with three oxygens on the alumina surface in groups of three iron atoms. This

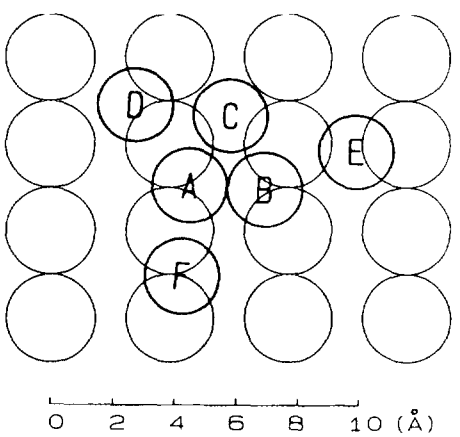

FIG. 7. Tentative model of Fe/Al_2O_3(K7) in accordance with a (110) plane and the EXAFS-derived results listed in Table 3.

constitutes a two-dimensional aggregating process. This process is favored by the surface structure of Al_2O_3 particles. Groups of Fe atoms in combinations other than three are less favored for geometrical reasons. The aggregation of iron trimers, but not the shortening of the Fe–Fe bonds, causes the decrease of the selectivity of the iron catalyst in the hydrogenation of carbon monoxide in this system. Although we have suggested that the presence of iron trimers is essential for the high selectivity of the fresh catalysts, the microenvironment surrounding the trimer seems to be at least equally important. For a highly dispersed iron catalyst such as K7, the active site is associated with an iron trimer that would show high selectivity only when no adjacent metallic group is present.

CONCLUSION

Precipitating $Fe_3(CO)_{12}$ on alumina is a successful method for the preparation of highly dispersed supported cluster and cluster-derived iron catalyst. The structural characterization of the iron catalysts by *K*-edge EXAFS analysis suggests that the Fe_3 cores of some of the $Fe_3(CO)_{12}$ molecules are retained on the alumina surface in the catalyst Fe/Al_2O_3. In addition, some isolated iron atoms are also formed on the freshly prepared catalyst. For the catalytic hydrogenation of CO, the active site on the alumina surface appears to be associated with the iron trimers. However, it will present a high selectivity under the condition that the iron trimer is accompanied by a "clean" microenvironment with only isolated iron atoms nearby.

ACKNOWLEDGMENTS

This work is part of a project supported by the National Natural Science Foundation (NNSF), China. We are grateful to the Photon Factory in Tsukuba, Japan, for support and use of the BL-10B and BL-7C facilities. One of us (Y.K.) thanks the Takasago Research Institute, Inc., and Dr. S. Akutagawa, and another of us (M.T.) thanks the Department of Chemistry, Hokkaido University and Professor K. Tanabe for hospitality and support. We are indebted to Professor John J. Rehr and his colleagues of the Department of Physics, Uni-

versity of Washington, for the use of their program FEFF3.25.

REFERENCES

1. Zwart, J., and Snel, R., *J. Mol. Catal.* **30,** 305 (1985).
2. Stevenson, S. A., Goddard, S. A., Arai, M., and Dumesic, J. A., *J. Phys. Chem.* **93,** 2058 (1989), and Refs. (7) to (15) therein.
3. Muetterties, E. L., Rhodin, T. N., Band, E., Brucker, C. F., and Pretzer, W. R., *Chem. Rev.* **79,** 91 (1979).
4. Hugues, F., Basset, J. M., Ben Taarit, Y., Choplin, A., Primet, M., Rojas, D., and Smith, A. K., *J. Am. Chem. Soc.* **104,** 7020 (1982).
5. Dry, M. E., *in* "Applied Industrial Catalysis" (B. E. Leach, Ed.), Vol. 2, P. 190. Academic Press, San Diego 1983.
6. King, R. B., and Stone, F. G. A., *Inorg. Synth.* **7,** 193 (1963).
7. Rehr, J. J., Mustre de Leon, J., Zabinsky, S. I., and Albers, R. C., *J. Am. Chem. Soc.* **113,** 5135 (1991).
8. Mustre de Leon, J., Rehr, J. J., Zabinsky, S. I., and Albers,. R. C., *Phys. Rev. B* **44,** 4146 (1991).
9. Bunker, G., Hasnain, S., Sayers, D., eds., "Report on International Workshops on Standard and Criteria in XAFS, Proceedings, 6th International Conference on XAFS, York, England, 1990."
10. Lytle, F. W., Sayers, D. E., and Stern, E. A., *Phys. B* **158,** 701 (1989).
11. Cox, A. D., *in* "EXAFS for Inorganic Systems", p. 51. DL/SCI/R17, 1981.
12. Shriver, D. F., and Whitmire, K. H., *in* "Comprehensive Organometallic Chemistry" (G. Wilkinson, Ed.), Vol. 4, p. 260. Pergamon, Elmsford, NY, 1982.
13. Hugues, F., Smith, A. K., Ben Taarit, Y., and Basset, J. M., *J. Chem. Soc. Chem. Commun.*, 68 (1980).
14. Kou, Y., and Wang, H.-L., "Abstract, 7th International Symposium on Relations between Homogeneous and Heterogeneous Catalysis, Tokyo, Japan, 1992," p. 493.
15. Bianconi, A., Garcia, J., and Benfatto, M., "Topics in Current Chemistry," Vol. 145, p. 29. Springer-Verlag, Berlin, 1988.
16. Sano, M., *Inorg. Chem.* **27,** 4249 (1988).
17. Cotton, F. A., and Wilkinson, G., "Advanced Inorganic Chemistry," p. 752. Wiley, New York, 1980.
18. Cotton, F. A., and Troup, J. M., *J. Am. Chem. Soc.* **96,** 4155 (1974).
19. Binsted, N., Evans, J., Greaves, G. N., and Price, R. J., *J. Chem. Soc. Chem. Commun.*, 1330 (1987).
20. Knözinger, H., and Zhao, Y., *Faraday Discuss. Chem. Soc.* **72,** 53 (1981).
21. Deng, J.-Z., Wang, D.-Z., Wei, X.-M., Zhai, R.-S., and Wang, H.-L., *Surf. Sci.* **249,** 213 (1991).
22. Foger, K., *in* "Catalysis: Science and Technology" (J. R. Anderson and M. Boudart, Eds.), Vol. 6, Chap. 4, p. 231. Springer-Verlag, Berlin/New York, 1984.
23. Lippens, B. C., and de Boer, J. H., *Acta Crystallogr.* **17,** 1312 (1964).
24. Iijima, S., *Surf. Sci.* **156,** 1003 (1985).
25. Reller, A., and Cocke, D.L., *Catal. Lett.* **2,** 91 (1989).
26. Chen, Y., and Zhang, L., *Catal. Lett.* **12,** 51 (1992).